

Polynomial element velocimetry (PEV): A novel method for better than pixel resolution measurements

C. R. Samarage^{1,2}, J. Carberry^{2,3}, G. J. Sheard², A. Fouras¹

¹Division of Biological Engineering, Monash University,
Melbourne VIC 3800, Australia
rajeev.samarage@monash.edu

²Department of Mechanical and Aerospace Engineering, Monash University,
Melbourne VIC 3800, Australia

³Fluids Laboratory for Aeronautical and Industrial Research (FLAIR), Monash University,
Melbourne VIC 3800, Australia

ABSTRACT

A novel method utilizing a correlation-based approach for high-resolution velocity measurements is presented. Existing techniques for high-resolution velocity measurements use the modal velocity for estimating the displacement, and a wealth of information stored in the cross-correlation is discarded. A background study on optimizing the measurement accuracy of PIV in estimating the displacement and the gradient of the flow is presented. We introduce a novel method, which can yield velocity measurements that have infinite resolution, and the velocity gradient that is directly computable.

1. INTRODUCTION

Over the past two decades, Particle Image Velocimetry, or PIV, has gained popularity as a method for many experimental fluid mechanics investigations. Over this period, significant advances have been made to improve the spatial resolution and the accuracy of PIV measurements. The accuracy of PIV measurements have been shown to be affected by numerous factors ranging from correlation errors due to inadequate tracer seeding [1,2], to velocity gradients in the underlying flow [2] to name a few.

As the general PIV technique offers measurements that are discretized into sampling windows or interrogation windows, there lies a limit to which the size of a given sampling window can be reduced. At larger sampling window sizes, the spatial resolution to resolve specific structures in the flow is lost. At smaller window sizes, a loss of sufficient particle image pairs can lead to correlation errors leading to biased measurements. This results in a trade-off between the measurement accuracy and the spatial resolution of the measurements.

Existing techniques for high-resolution velocity measurements include hybrid PTV/PIV techniques [3], recursive local correlation [4], single-pixel evaluation techniques [5] and iterative multi-grid methods [6]. However, these methods use the modal velocity for estimating the displacement, and a wealth of information stored in the cross-correlation is discarded.

Other methods such as image deformation [7] have long been in use to improve the spatial resolution of PIV measurements while improving the measured velocity gradient. Recently, this technique has been applied to 3D volumetric data using a least squares matching algorithm [8]. Scharnowski et al, [9] showed recently that smearing of the cross-correlation with velocity gradients could be used to calculate the Reynolds stresses.

Recently, correlation-based least squares methods have been shown to utilize the depth information for 3D flow measurements [10, 11]. The underlying concept of these methods is that the cross-correlation map for a given window is the sum of the individual cross-correlation maps at each depth. The cross-correlation function in an interrogation window at a given depth is modeled as the convolution of the probability distribution of the displacement in that domain, and the auto-correlation of the particle image at that depth. To decode the depth information, Holographic Correlation Velocimetry [11] (also presented in this conference) uses the particle image diffraction pattern, while Volumetric Correlation Velocimetry [10] uses the out-of-focus effects on the particle image. While these methods are capable of offering high-resolution measurements in the out-of-plane axis, the measurements are still discretized into interrogation sub-regions in which the cross-correlation is calculated, and are subject to inaccuracies in estimating flow gradients.

We present a background study on optimizing the PIV measurement accuracy for estimating the displacement and flow gradient in Sect. 2. In Sect. 3, we present a novel method that can directly solve for an equation for the flow in a sampling window based on its cross-correlation map. The velocity components and its derivatives are readily available at an infinite resolution. In Sect. 4 we conduct a preliminary comparison of the novel method to PIV and a CFD solution for the flow around a square cylinder.

2. ANALYSIS OF PIV ACCURACY

With standard PIV, analysis or interrogation is conducted on a sequence of image pairs, where each pair is sub-divided to regions called sampling windows. This results in velocity measurements that are discretized to these sub-regions. High spatial resolution PIV measurements can be obtained in two ways: reducing the sampling window size, and overlapping sampling windows to further improve resolution.

A Monte Carlo simulation using synthetic images was conducted to study the PIV measurement accuracy in estimating the displacement as functions of the sampling window size and window overlapping. Synthetic images of resolution $2,048 \times 2,048$ px² were generated for a Lamb-Oseen vortex flow [12], where the in-plane tangential velocity and out-of-plane vorticity field is given by:

$$u_t(r) = \frac{\Gamma}{2\pi\tau} \left[1 - \exp\left(\frac{-r^2}{4vt}\right) \right] \quad (1)$$

$$\omega_z(r) = \frac{-\Gamma}{4\pi\nu t} \exp\left(\frac{-r^2}{4\nu t}\right) \quad (2)$$

where $r^2 = X^2 + Y^2$ and (X, Y) are global in-plane Cartesian coordinates, Γ is the circulation, ν is the kinematic viscosity and t is time. The size of the Oseen vortex, L , is defined as

$$L = \sqrt{4\nu t} \quad (3)$$

The numerical analysis has been conducted for a circulation, Γ , of 1,000 px²/s and a core vortex diameter, L , of 200 px. All images are generated with 256 gray levels and a pixel fill factor of 0 (i.e. gray value sampled at the center of the pixel).

The error in the measurement is the difference between the estimate from PIV and the analytical solution from equations 1 and 2. The sampling window size, W , is varied from 8 px to 256 px. Varying the sampling distance, Δ , varies the window-overlap ratio and is varied from 8 px to 256 px. Figure 1 shows a line plot of the RMS of the PIV error in estimating the velocity components, u and v , as a function of sampling window size, W . Decreasing window size increases the error in the measurement as there is a loss of correlation due to the smaller window sizes; while increasing window size increases the error since the structure of the flow cannot be resolved. The RMS error is optimal when the sampling window size is 64 px. Only the plot for a sampling distance of 8 px is shown, as there is minimal variation to the RMS error with increasing sampling distance.

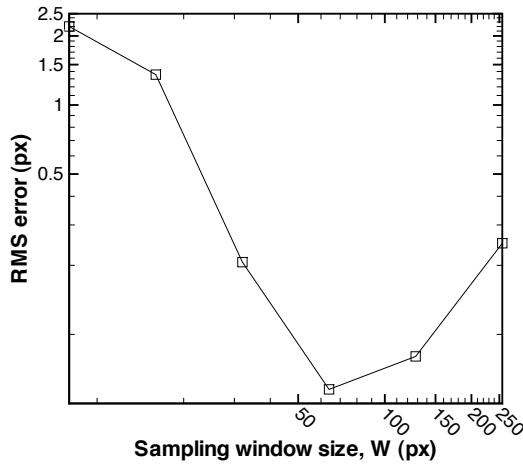


Figure 1: RMS of the PIV error in estimating the velocity components, as a function of the sampling window size, W , for a sampling distance, Δ , of 8 px.

Another important measurement is the vorticity field, which can be computed directly from the velocity field. Figure 2 shows a contour plot of the RMS of the PIV error in estimating vorticity, as a function of sampling window size, W , and the sampling distance, Δ , normalized to the vortex size, L . The vorticity field is calculated using the method discussed by Fouras and Soria [13].

In figure 2, when the sampling distance is 8 px, i.e. when $\Delta/L = 0.04$, the RMS error is optimal at a window size of 64 px ($W/L = 0.32$). This agrees with the result for the velocity component in figure 1. There is almost no variation in the error below $\Delta/L \sim 0.16$, sampling window size alone

optimizes the vorticity accuracy. However, as the sampling distance is increased further, sampling window size as well as the sampling distance optimizes the vorticity measurement as the number of data points in estimating the vorticity decreases.

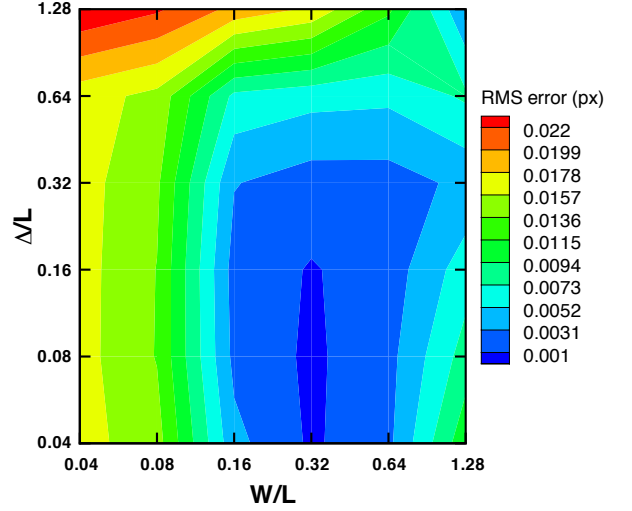


Figure 2: RMS of the error in estimating the vorticity (contours), as a function of the sampling window size, W , and the sampling distance, Δ , normalized to vortex size, L . The accuracy of estimating vorticity is optimized with sampling window size as well as offset.

We can see that with PIV, the accuracy of the measurement is affected by the resolution, especially in estimating the flow gradients from the velocity field. In this paper, we propose a novel cross-correlation based method, which uses a least-squares solver to solve for a polynomial equation that describes the flow within each sampling window. This polynomial can then be directly used to determine flow gradients with infinite resolution.

2. THE NOVEL METHOD

A novel method to directly determine a piece-wise grid of two-dimensional polynomials, which describes the entire flow field, is presented. The method, which we term 'Polynomial Element Velocimetry' or PEV, solves for a tensor-product of cubic polynomials by modelling an estimate for the cross-correlation map and performing a non-linear minimization with the measured cross-correlation map obtained from standard PIV. Figure 3 shows a graphical representation of the steps involved in the PEV method. The steps involved are as follows:

- 1) The overall flow field is discretised into a grid of regular regions called 'elements', which are analogous to sampling windows used in PIV. Standard PIV with smaller sampling windows is conducted within the larger elements to fit a first approximation of the polynomials describing the flow over each element.
- 2) For each element, the polynomial equations for the u and v -components of velocity are used to construct a probability distribution function (PDF), P , for the underlying flow. This function is convolved with the element's corresponding measured auto-correlation function, A , to obtain an estimate for the cross-correlation map, C , as shown in equation 4.

$$C_{est}(x, y) = P(x, y) * A_{meas}(x, y) \quad (4)$$

- 3) The estimate for the cross-correlation map is compared to the measured cross-correlation map determined within the element from standard PIV. The polynomial for the flow is refined, and processes 2 and 3 are repeated until the error between the estimated cross-correlation map and the measured cross-correlation map is minimised.

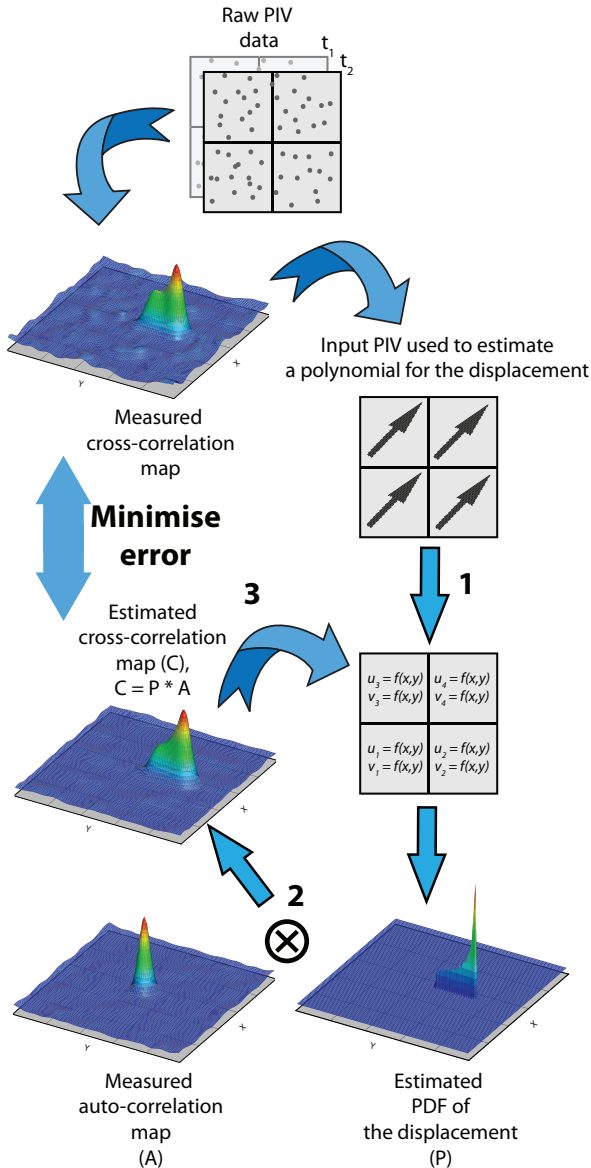


Figure 3: Graphical representation of the PEV algorithm. This novel method minimises the measured cross-correlation map from raw PIV data to determine a polynomial that defines the flow. Displacement measurements from PIV data are used as estimates to the PEV method (1). Polynomials that define the displacement inside an element in x and y, are used to model a probability distribution function (PDF) of the displacement within the element, P. The PDF is then convolved with the auto-correlation of the element, A, to obtain the model cross-correlation, C (2). This process is iterated until the error between the modelled and the measured cross-correlation maps is minimised (3).

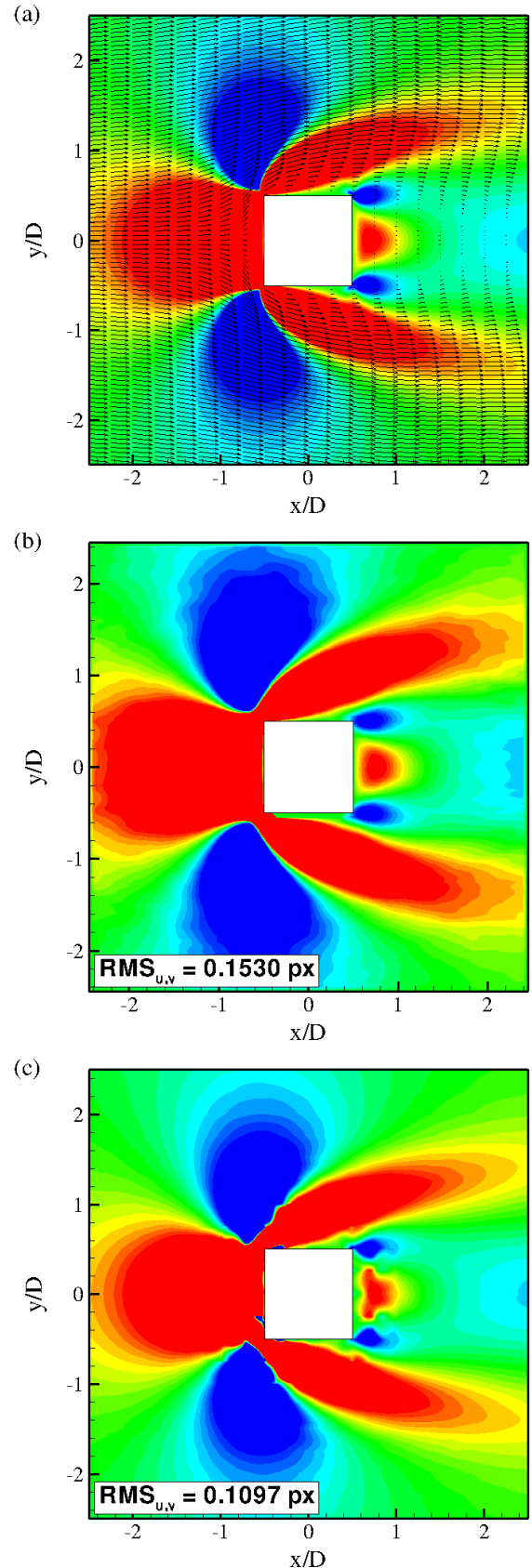


Figure 4: Contour plots for the flow gradient, dv/dy for the flow behind a square cylinder at a Reynolds's number of 30, as obtained from (a) the CFD solution, (b) standard PIV and (c) the PEV method.

The solver uses a Levenberg-Marquardt [14] non-linear least squares solver to perform the error minimization described in step 3). Steps 2 and 3 are performed for each element until the error is minimized for the entire field. Since the flow should be continuous through the elements, a Tikhonov regularisation method [15] is employed during the error minimization process. This method adds weightings to minimise discontinuities in both the velocity components and their spatial derivatives at element interfaces.

3. APPLICATION TO SYNTHETIC DATA

To validate the accuracy of the novel PEV method, synthetic 300 image pairs of resolution $1,000 \times 1,000 \text{ px}^2$ were generated for the flow around a square cylinder at a Reynold's number of 30. The particles were displaced based on a CFD solution that was computed using in-house software. The keen reader is referred to the paper by Sheard et al., [16, 17], for further information on the CFD software used in this paper. Figure 4a shows the CFD solution data used for validating the novel PEV process. The contours show the velocity gradient dv/dy , while the vectors show the velocity. Only results in estimating the velocity gradients are shown in the following plots, as it is more sensitive to error, and hence can highlight discrepancies in either the calculated or measured velocity fields.

The tracer particles used were assumed to be ideal and have a Gaussian shape with a particle diameter of 3 px. The pixel fill factor is 0. An element is $50 \times 50 \text{ px}^2$ in size, and the entire field consists of 20×20 elements.

Since the polynomial for the flow is known in each element, the derivatives are readily computable. Figure 4b shows the flow gradient, dv/dy , computed by the method proposed by Fouras and Soria [13]. The PIV velocity measurements were estimated using a correlation average of 300 image pairs, with a sampling window size of $50 \times 50 \text{ px}^2$, and a window overlap of 50% (i.e. a sampling distance of 25 px). The RMS PIV error in estimating the u and v components of the velocity compared to that of the CFD solution in figure 4a is approximately 0.15 px. Figure 4c shows the contour plot for the gradient, dv/dy , computed using the proposed PEV method. The flow field for PEV is defined over 20×20 elements. The RMS error in estimating the components for velocity using in PEV is approximately 0.11 px. The percentage reduction in error from PIV to PEV is approximately 33%. The high spatial resolution of the measurements using PEV over PIV is clearly evident. Albeit minor irregularities in the estimated flow gradient due to aggressive ridge regression techniques, the PEV method estimates the gradient much more accurately. Small but significant features of the flow are visible with the velocity gradients measured using the proposed PEV method. These features include the flow directly behind the cylinder, and the smoothness of the flow gradient contours.

4. CONCLUSIONS

A novel process that yields a two-dimensional cubic polynomial to represent the flow is presented. This process, which we term Polynomial Element Velocimetry (PEV), solves for the said polynomial by modelling an estimate for the cross-correlation map and performing a non-linear minimization with the measured cross-correlation map obtained from standard PIV. This technique models the cross-correlation map as the convolution of the auto-correlation of the particle image pair and the probability distribution of the

displacement (Eq. 4) [10, 11]. This concept ensures that the PEV method optimally uses all the in-plane flow information in the cross-correlation map over the standard PIV process that yields the modal velocity.

Once the two-dimensional cubic polynomials for the velocity are known, the velocity and the velocity gradient are directly calculable. Hence, this new method allows for accurate velocity measurements near a wall and the accurate location of flow features such as stagnation points, over current methods.

ACKNOWLEDGMENTS

The authors would like to acknowledge the insightful discussions with Stephen Dubskey. Support from the Australian Research Council under Discovery Grant DP0987643 is gratefully acknowledged. C.R.S. is a recipient of an Australian Postgraduate Award.

REFERENCES

- [1] Keane R.D. & Adrian R.J. (1990) Optimization of particle Image velocimeters: I. double pulsed systems. *Meas. Sci. Technol.* **1**. 1202-1215
- [2] Keane R.D. & Adrian R.J. (1992) Theory of cross-correlation analysis of PIV images. *Appl. Sci. Research.* **49**. 191-215
- [3] Stitou A. & Riethmuller M. L., (2001) Extension of PIV to super resolution using PTV, *Meas. Sci. Technol.*, **12**. 1398-1403
- [4] Hart D. P. (1999) Super-resolution PIV by Recursive Local-Correlation, *Jour. Visualization*, **10**. 1-10
- [5] Westerweel J., Geelhoed P. F. & Lindken R., (2004) Single-pixel resolution ensemble correlation for micro-PIV applications, *Exp. Fluids*, **37**. 375-384
- [6] Scarano F. & Riethmuller M.L. (1999) Iterative multigrid approach in PIV image processing with discrete window offset, *Exp. Fluids.*, **26**. 513-523
- [7] Scarano F. (2002) Iterative image deformation methods in PIV, *Meas. Sci. Technol.*, **13**. R1-R9
- [8] Westfield P., Maas H-G., Pust O., Kitzhofer J. & Brucker C. (2010) 3-D least squares matching for volumetric velocimetry data processing, *In Proc. 15th Int Symp on Applications of Laser Techniques to Fluid Mechanics*, Lisbon, Portugal, 05-08 July
- [9] Scharnowski S., Hain R. & Kahler C. J. (2010) Estimation of Reynolds Stresses from PIV Measurements with Single-Pixel Resolution, *In Proc. 15th Int Symp on Applications of Laser Techniques to Fluid Mechanics*, Lisbon, Portugal, 05-08 July
- [10] Fouras A., Lo Jacono D., Nguyen C.V. & Hourigan K. (2009) Volumetric Correlation PIV: a New Technique for 3D Velocity Vector Field Measurement, *Exp. Fluids*, **47** (4). 569-577
- [11] Higgins S.P.A, Samarage C.R., Paganin D.M. & Fouras A. (2011) Holographic Correlation Velocimetry, *In Proc. 9th Int Symp on Particle Image Velocimetry*, Kobe, Japan, 21-23 Japan
- [12] Saffman P. (1995) *Vortex Dynamics*, Cambridge University Press
- [13] Fouras A. & Soria J. (1998) Accuracy of out-of-plane vorticity measurements derived from in-plane velocity field data, *Exp. Fluids*, **25**. 409-430
- [14] Marquardt D. (1963) An algorithm for least-squares estimation of nonlinear parameters, *SIAM Journ. on Appl. Math.*, **11** (2). 431-441

- [15] Tikhonov A. N., (1963) Solution of incorrectly formulated problems and the regularization method, *Sov. Math. Dokl.*, **4**. 1035-1038
- [16] Sheard G. J., Fitzgerald M. J., & Ryan K., (2009) Cylinders with square cross section: Wake instabilities with incidence angle variation, *J. Fluid Mech.*, **630**. 43-69
- [17] Sheard G. J., (2011) Wake stability features behind a square cylinder: Focus on small incidence angles, *J. Fluids. Struct. (in press)*. DOI: 10.1016/j.jfluidstructs.2011.02.005